DEVELOPING METHODS FOR PERINATAL HEALTH SCREENING

By

JENNIFER PISERCHIA

BS, THE COLLEGE OF NEW JERSEY, 2019

Thesis

Submitted in partial fulfillment of the requirements for the Degree of Master of Science in the Graduate Program of Biomedical Engineering at Brown University

PROVIDENCE, RHODE ISLAND

MAY 2024

AUTHORIZATION TO LEND AND REPRODUCE THE THESIS

As the sole author of this thesis, I authorize Brown University to lend it to other institutions for the purpose of scholarly research.

Date_____ _____

JENNIFER PISERCHIA, Author

I further authorize Brown University to reproduce this thesis by photocopying or other means, in total or in part, at the request of other institutions or individuals for the purpose of scholarly research.

Date_____ _____

JENNIFER PISERCHIA, Author

This thesis by Jennifer Piserchia is accepted in its present form by the Center for Biotechnology as satisfying the thesis requirements for the degree of Master of Science

Date_____ Signature: _____

Dr. ANUBHAV TRIPATHI, Advisor

Date_____ Signature: _____

Dr. THERESA RAIMONDO, Reader

Date_____ Signature: _____

Dr. GARY WESSEL, Reader

Approved by the Graduate Council

Date_____ Signature: _____

Dr. Thomas A. Lewis, Dean of the Graduate School

Acknowledgements

I would like to express my deepest gratitude to Dr. Anubhav Tripathi for his support and encouragement throughout my time at Brown and for granting me with the opportunity to perform research in a field I'm so passionate about. I'd also like to thank my committee members, Dr. Theresa Raimondo and Dr. Gary Wessel, for their patience, time, support, and guidance throughout the course of my thesis. A sincere thanks to Dr. Marissa Gray for her mentorship, support, and encouragement through pivots in my research. Many thanks to Revvity for providing funding and technical support for this work.

Thank you to all my professors at Brown, not only for all the lessons I learned in their classes, but also for inspiring me to pursue my highest career aspirations and passions, despite challenges I may face. The experiences I had taking classes at Brown were rewarding and enriching, made me excited to learn, and most of all, grateful to be here.

I'm extremely grateful to my mentor, Jennifer Pollock, for her daily support on these projects. Without her guidance and mentorship, I wouldn't have been able to pick up so many new skills in such a short time. It's because of her challenging me every day that I'm able to graduate from Brown feeling accomplished in new areas of science and engineering. I'd also like to extend my gratitude to Adriana Coll de Peña, who laid more than the groundwork for the aneuploidy project. An additional thanks goes to Christine Lujuo along with Jennifer Pollock, who were supportive in taking on preeclampsia for one of our course projects and worked with me to further develop the idea. Thank you to Allistair Yu for writing a custom MATLAB code to streamline data analysis.

I would be remiss in not mentioning Stephanie Roser, who continuously motivated me not only throughout my thesis, but also prior to my matriculation at Brown. She encouraged me every

step of the way, always offering to help where she could, and answering my questions with patience and kindness. I'd also like to acknowledge Stephanie Roser & the Coulombe lab for allowing me to use their pH probe for one of my experiments.

I'd like to express my appreciation to Stryker along with my colleagues, leadership, and HR team there for their willingness to find a solution that allows me to work and pursue higher education. Their support, flexibility, and patience have allowed me to continue to develop as an engineering professional while expanding technical competencies in new fields.

Of course, very special thanks to my family for their ongoing support in every stage of my career. To my parents, Ellen and John, my brother, Daniel, and my partner, Kevin: I can't thank you enough for the love and support you have provided during this time. Kevin – I will never stop being grateful for the way you empower me to pursue my dreams, even on the hardest days, but I can start by saying thank you.

Table of Contents

Table of Figures

Table of Tables

Abstract of DEVELOPING METHODS FOR PERINATAL HEALTH SCREENING, by JENNIFER PISERCHIA, ScM, Brown University, MAY 2024.

Screening for maternal and prenatal health conditions allows for better patient care and improved health outcomes. In maternal health, hypertensive conditions like preeclampsia, which leads to an increased risk for a number of fatal complications, lack specific and sensitive screening tools. In fetal health, chromosomal abnormalities are a primary concern during development, but standard diagnostic test methods carry a risk of miscarriage, therefore there is a need for a noninvasive screening method for aneuploidy. In response to the need for new screening tools for preeclampsia and aneuploidy, two perinatal screening methods were developed: a dual-bead based assay to screen for preeclampsia and an automated capillary electropherogram based assay to screen for aneuploidy. The dual-bead assay relies on an antibody-carbohydrate sandwich used to capture sFlt-1, a protein biomarker for preeclampsia, for detection using qPCR. The aneuploidy screening method uses modified cfDNA and probes to bind DNA fragments for a non-quantitative, size based detection of aneuploidy. Experiments were unable to be executed for the preeclampsia study, but expected results are detailed. For the aneuploidy study, a series of experiments were performed to optimize a double DNA hybridization using model cfDNA and DNA probes. Results showed that preparing samples with a pH of 6 is optimal for hybridization. Future work should be done at a higher sample size to verify these results. A novel method to screen for aneuploidy in a non-invasive and non-quantitative way is presented.

Chapter 1: Introduction

Maternal morbidity and mortality rates in the United States are the highest out of the developed nations, despite having an advanced health system[1]. Some causes of the rise in maternal morbidity are systemic, requiring health care reform. In 2022, the Biden-Harris administration announced a call to action on maternal health with the goal of improving parental and infant health outcomes[2]. Other causes are advanced maternal age and chronic health conditions, such as heart disease, stroke, and hypertension[3]. Improving diagnostic measures can allow doctors and patients to intervene early and provide better care to patients. With that in mind, there are two conditions that this research thesis focuses on: preeclampsia and aneuploidy.

There are a number of prenatal tests that are done during the course of a pregnancy. Some tests are performed to monitor the health of the mother and fetus while others are performed to identify birth defects and genetic conditions[4]. For example, blood pressure measurements are regularly taken to assess for hypertensive disorders; this is a monitoring test. Genetic testing, on the other hand, is only performed once or twice to diagnose genetic conditions like aneuploidy. Both of these conditions have the potential to vastly influence the outcome of the pregnancy, so it is imperative to screen and diagnose early and accurately.

Preeclampsia

Hypertensive disorders contribute to obstetric complications in 10% of pregnancies. Out of the hypertensive disorders, including gestational hypertension and chronic hypertension, preeclampsia is the most fatal. Preeclampsia is a pregnancy specific disorder characterized by hypertension and proteinuria that affects 7% of pregnancy-related maternal deaths. Pre-eclampsia increases the risk of fetal growth restriction, preterm birth, cesarean delivery, and long-term cardiovascular disease. Its highest prevalence is among women older than 35 years and women of Black (20.9%) or American Indian and Alaska Native heritage (16.4%)[5].

Detecting pre-eclampsia early is important for early initiation of medical care. Preeclampsia often develops in the third trimester but can develop as early as 20 weeks and as late as six weeks after birth[6].

Preeclampsia is currently diagnosed by blood pressure readings and urinalysis. Platelet numbers and further liver and kidney function may be evaluated as well. Primary diagnostic criteria after 20 weeks include systolic blood pressure ≥140 mm Hg or systolic blood pressure ≥90 mm Hg on more than two occasions 4 hours apart or ≥160/110 mm Hg at a shorter time interval. Proteinuria and signs of end-organ damage may also be present and used as diagnostic criteria[7]. Although this diagnostic criteria is used, it combines qualitative and quantitative assessments and can lead to misdiagnosis, with one study finding a misdiagnosis rate as high as 31%[8]. Additionally, these criteria cannot be used for the early diagnosis of preeclampsia. Despite the risk of misdiagnosis and late diagnosis, there is no one gold standard test for the diagnosis of preeclampsia. One cause for delays in the development of a gold standard test is understanding the mechanisms causing preeclampsia.

Some theories on preeclampsia's etiology focus early in fetal development, when the zygote produces villi that attach to the uterine lining. Uterine blood vessels, called spiral arteries, provide nutrients to the villi, allowing it to develop into the placenta. Spiral arteries undergo remodeling in the early stages of pregnancy to allow for high-flow, low-resistance placental circulation. This remodeling is vastly important for placental development since maternal blood volume and placental blood flow increases in normal pregnancy development[9]. In the case of preeclampsia, spiral arteries fail to remodel appropriately[10]. This causes one of the landmark indicators of preeclampsia: hypertension.

This theory is further supported by molecular mechanisms where antiangiogenic and proangiogenic proteins play a role. Previous studies have demonstrated that an imbalance in these proteins in maternal circulation is created by cellular ischemia in the placenta of patients with preeclampsia[11]. Soluble Fms-like tyrosine kinase-1 (sFlt-1) is an antiangiogenic protein and spliced variant of vascular endothelial growth factor (VEGF) receptor that binds VEGF and placental growth factor (PlGF). Because of its antiangiogenic properties, it reduces blood vessel growth through its high affinity binding to VEGF and PlGF[12]. VEGF/VEGFR family of growth factors and receptors play a role in angiogenesis and vasculogenesis and since the disruption of vascular endothelial function is a known feature of preeclampsia, sFlt-1 binding VEGF may provide a cause for this dysfunction. PlGF is similarly a proangiogenic factor that affects feto-placental circulation and trophoblast growth[13]. Thus, sFlt-1 binding to PlGF would disrupt circulation and trophoblast growth. Through these mechanisms, sFlt-1 has the capacity to cause the widespread endothelial dysfunction associated with preeclampsia[14].

sFlt-1 has been found in elevated concentrations in the maternal serums of patients with preeclampsia, even when clinical symptoms of preeclampsia are not significant. After the onset of preeclampsia, patients had levels of sFlt-1 at 51.9 ng/mL compared to controls with 13.6 ng/mL of sFlt-1[15]. Because of these elevated values, sFlt-1 serves as a promising biomarker for preeclampsia.

Heparin is known to tightly bind Flt1, a protein that is abnormally expressed in preeclampsia[15]. sFlt-1 has a heparin binding site that binds heparin with a high affinity. Antibodies against sFlt-1 are also able to bind to sFlt-1 with high specificity. By leveraging the high binding affinity of heparin and the high specificity of anti-sFlt-1 antibodies, an antibody-

carbohydrate sandwich can be formed to capture sFlt-1 protein molecules and measure their concentration in serum.

The goal of this study is to create a novel quantitative screening method for preeclampsia.

Aneuploidy

Aneuploidy is a genetic disorder in which there is a chromosomal abnormality that results in the presence or absence of a chromosome. Aneuploidy is the leading cause of miscarriages and congenital birth defects, with aneuploidy and polyploidy present in 96% of chromosomal abnormalities in miscarriages[16]. In these cases, chromosomes 13, 16, 18, 21, 22, X, and Y are most frequently involved. Trisomy 21 is the most common aneuploidy to result in a live birth while monosomy X and trisomy 16 are the most common aneuploidy to cause miscarriage[17].

The precise etiology of aneuploidy is unknown, however it is theorized that it primarily occurs through nondisjunction in the first meiotic division[17]. Numerous studies have also reported a correlation with advancing maternal age and incidence of aneuploidy. Other studies have explored the potential influence of paternal factors on aneuploidy but no association was found[18].

The gold standard, conventional diagnostic test for aneuploidy is karyotyping. However, this method has an overall failure rate of 21%[16]. This testing also relies on chorionic villus sampling from amniotic fluid, which is associated with a 0.1-0.3% risk of infection and 0.5% risk of miscarriage[19]. Alternatives such as fluorescence in situ hybridization (FISH) have been found to report biologically implausible levels of aneuploidy, raising the question of the test's accuracy[20]. Noninvasive prenatal screening (NIPS) methods have emerged as a new method to screen for aneuploidy, demonstrating higher specificity and sensitivity than traditional screening methods for Patau, Edwards, and Down syndromes[21]. There are a variety of NIPS techniques

used to screen for aneuploidy including massively parallel shotgun sequencing, targeted massively parallel sequencing, single nucleotide polymorphism, polymerase chain reaction with restriction enzyme digest, and next generation sequencing[22]. These methods typically use maternal serum to detect aneuploidies in chromosomes 13, 18, and 21.

Specifically, NIPS relies on the fetal fraction to predict aneuploidy. Fetal fraction is the amount of DNA in maternal circulation that originates from the fetus. The combination of maternal and fetal DNA make up cell-free DNA. Cell-free fetal DNA (cfDNA), shed by the placenta, is typically made up of fragments sized 50-300 base pairs long. When there is an extra chromosome present, as in trisomy, fetal fraction will increase, proportional to the size of the chromosome. Because of this, a higher fetal fraction is indicative of a higher chance of aneuploidy. Fetal fraction can range from 4-30%, but a minimum of 4% is typically required for aneuploidy detection through NIPS methods. NIPS methods that rely on fetal fraction quantification include methylation differences, SNP quantification, length distribution, and Y chromosome, all of which come with their own pros and cons. None of these methods are both accurate and easy to perform[19]. There is a need for an accurate NIPS method that is easy to perform and inexpensive.

A novel method using rolling circle replication has been developed that relies on molecular probe technology that target chromosomes and a nanofilter based readout that allows for imaging and counting without DNA amplification, microarrays, or sequencing. This method, called the Vanadis noninvasive prenatal testing (NIPT) assay, is highly accurate and can detect aneuploidy with a fetal fraction as low as 2%. Figure 1 shows the workflow for this assay. In this process, cfDNA is extracted from maternal plasma from which target fragments are captured and converted into DNA circles. These fragments contain chromosomal information. DNA circles

are modified with a chromosomal tag for detection and quantification downstream in the process. Specific probes and backbones are hybridized to the DNA circles, there is a cleanup step, and then rolling circle replication is performed to amplify the signal. Chromosome tags are labeled with a fluorophore and then samples can be imaged. Aneuploidy could then be detected by the ratio of chromosomes present, performed using quadratic regression in the imaging software.

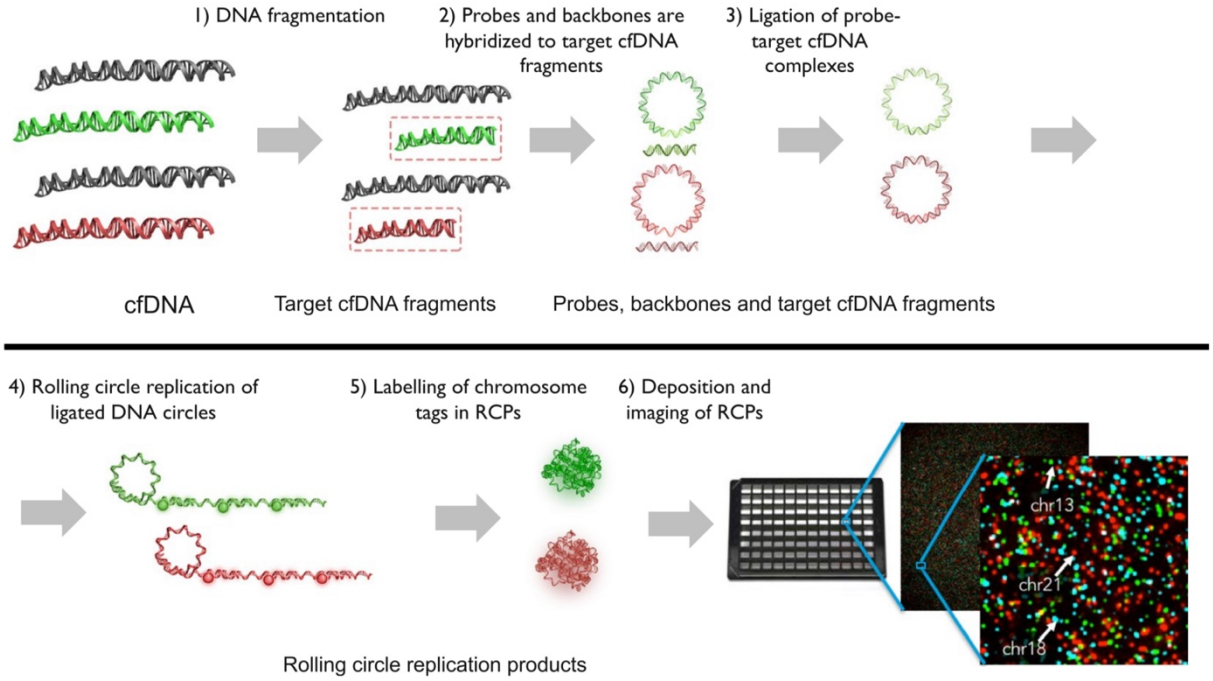

Figure 1. Vanadis NIPT Workflow adapted from Dahl 2017[23]

Although this test is specific and accurate, it has an extensive analytical requirement with the need to quantify fragments. The proposed changes to this test, as outlined in this thesis, allow for a high throughput and low-cost screening alternative. Microfluidic gel electrophoresis' inherent purification during analysis eliminates the need for an additional purification step in the workflow. Using a threshold-based screening method, there is also no need for quantification or labeling of fragments. These analytical simplifications reduce the cost and time required to execute this screening test, without sacrificing accuracy.

To simplify the workflow and negate the need for quantification downstream, it is proposed that no chromosomal tag is added and instead the DNA circles specific to chromosome 18 and 21 are modified with complementary, randomized 10 base pair overhangs. This is represented in Figure 2.

After linearization, the single stranded cfDNA backbones can be hybridized to specific probes, leaving only the overhang region unbound. During a second hybridization, the overhangs can then bind to each other, producing a long double stranded product that can be detected using microfluidics. Since chromosomes always come in pairs, a normal sample will always have this long product formed. If there is the presence of an extra chromosome or the absence of one, there will be a significant amount of unbound double stranded DNA that is detectable using size-based analysis. This would indicate aneuploidy, as shown in Figure 3.

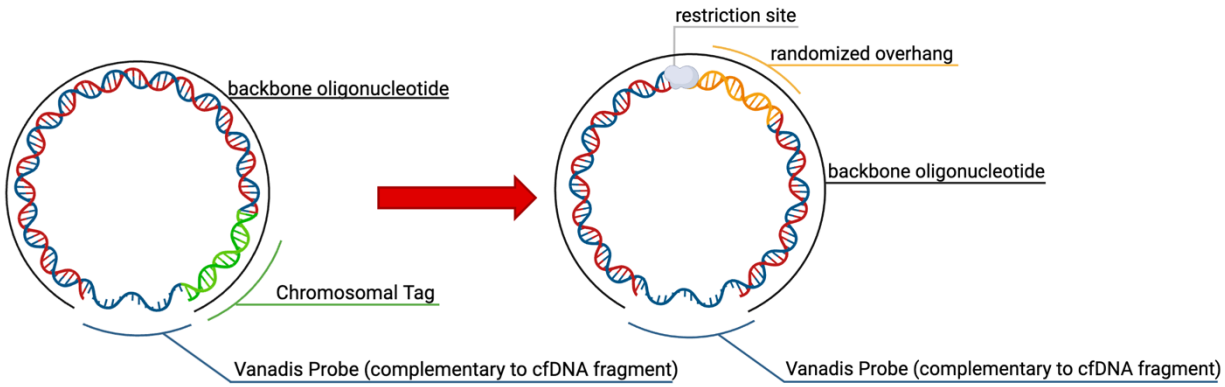

Figure 2. Proposed changes to cfDNA. Adapted from Dahl, et al. and created using BioRender.com[23]

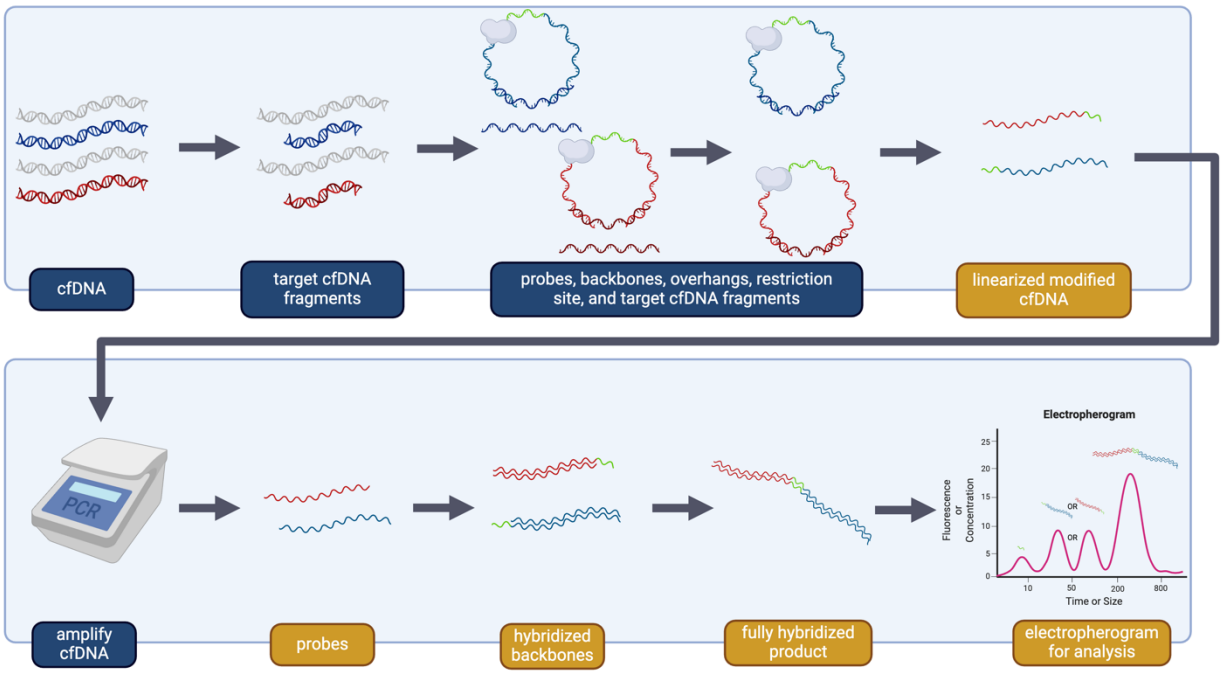

Figure 3. Proposed changes to Vanadis workflow. Steps tested in this thesis highlighted in gold. Created with BioRender.com

To test this theory, a model was created using four DNA backbones. Within these backbones, two represent model cfDNA while the other two represent probes. Model cfDNA has a randomized overhang region for binding to the complementary binding region on the other strand. DNA sequences were selected based on known sequences for chromosomes 18 and 21, designed so that one model cfDNA could represent chromosome 18 with a randomized overhang and one model cfDNA could represent chromosome 21 with a complementary overhang.

Microfluidic analysis allows for samples to be analyzed quickly and accurately. Automated microfluidic capillary electrophoresis technology combines microfluidic analysis with traditional gel electrophoresis to simplify the workflow and provide a robust analysis quickly. In the proposed workflow, automated microfluidic capillary electrophoresis is used to measure the DNA products created by this method. The output is an electropherogram, from which aneuploidy can be determined based on whether or not the ratio of peaks meets a predetermined threshold.

There are a number of models and mechanisms that impact nucleic acid migration. Nucleic acid size is the primary factor that influences electrophoretic mobility, as larger molecules will move slower and smaller molecules will move faster through the gel. Pore size of the gel matrix, electric field strength, and interactions between the gel matrix and sample will also have an impact on migration. It is also interesting to note that previous work has demonstrated the ability of double stranded RNA to migrate faster than single stranded RNA as fragment size increased[24].

In capillary electrophoresis, smaller molecules are able to be analyzed faster and with more accuracy than traditional slab electrophoresis. Samples are separated depending on the velocity of their individual components. This velocity (v) is controlled by the electrophoretic mobility (μ_e) of the sample and the electric field (E) applied[25].

$$v = \mu_e E$$

The electrophoretic mobility is dictated by a variety of equations and factors, which are detailed below.

$$\mu_e = \frac{E_f}{F_f}$$

Where E_f is electrical force exerted on the particle and F_f is frictional drag the gel matrix exerts on the particle.

$$E_f = qE$$

Where q is the charge of the ion.

$$F_f = -6\pi\mu\eta r v$$

Where r is the ion radius and η is the viscosity of the solution.

As shown by these equations, ions have a large effect on the ability of a sample to move through the gel matrix and should be explored as a potential avenue to enhance hybridization.

The goal of this study is to maximize the binding efficiency of the overhangs during the second hybridization, primarily through changes to the ionic strength of the sample buffer.

Chapter 2: Preeclampsia

METHODS

Materials

Superparamagnetic streptavidin coated Dynabeads M-270® (2.8 um, 10 mg ml^{-1}), Thermo Scientific™ EZ-Link™ NHS-PEG4-Biotin, Taqman® MGB Probe, UltraPure™ DNase/RNase-Free Distilled Water, and human plasma-like medium (HPLM) were selected for purchase from ThermoFisher Scientific. Recombinant human VEGFR1/Flt-1 Fc Chimera Protein and Human VEGFR1/Flt-1 Antibody were selected for purchase from R&D Systems. The ssDNA "tag", primers, and Heparin-immobilized beads (Heparin Sepharose: 6 Fast Flow 17-0998-01) were selected for purchase from Millipore Sigma.

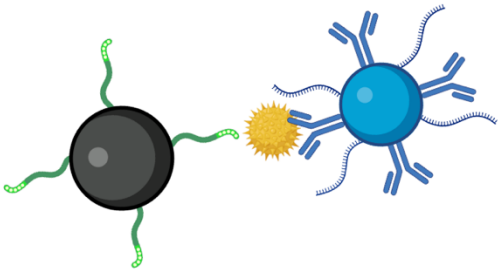

Figure 4. Heparin immobilized magnetic bead – target protein – polystyrene bead complex. The magnetic bead is immobilized with heparin and the polystyrene bead is functionalized with Flt-1 antibody and DNA tag. The Flt-1 protein would bind specifically to the antibodies on the polystyrene bead and non-specifically to the heparin on the magnetic bead. Created with BioRender.com.

Antibody Biotinylation Protocol

The lyophilized antibodies are reconstituted using PBS to a concentration of 0.5 mg ml^{-1}. The NHS-PEG_4-Biotin is reconstituted to a 20mM concentration using UltraPure™ DNase/RNase-Free Distilled Water. A 20-fold molar excess of biotin is added to the antibodies and allowed to react at room temperature for 30 minutes. Excess biotin is removed using an

Amicon Ultra-0.5 Centrifugal Filter Unit to remove the supernatant. The final antibody concentration is measured using the NanoDrop® ND-1000 UV-Vis Spectrophotometer.

Magnetic Bead Preparation Protocol

3 mg of 1.5 um Absolute Mag™ Heparin Silica Magnetic Particles are washed repeatedly using a wash buffer solution and centrifuged for three minutes at 13100 rpm. After the final wash and centrifuge, the solution is resuspended to a concentration of 5 mg ml^{-1} in PBS. Heparin is added to the solution and incubated at room temperature for 30 minutes with gentle mixing. The functionalized microbeads are then washed using the wash buffer and centrifuged a total of three times.

Polystyrene Bead Preparation Protocol

0.2 mg of 200 nm streptavidin coated polystyrene beads (~1.56 x 10^9 beads) are washed repeatedly with the wash buffer and centrifuged for 10 minutes at 13100 rpm. After washing, the solution is suspended as 1 mg ml^{-1} in PBS. Biotinylated human Flt-1 antibody is added to the solution and incubated at room temperature for 30 minutes with gentle mixing. The solution is then centrifuged for 10 minutes at 13100 rpm, the supernatant removed, and resuspended as 4 mg ml^{-1} in PBS. The biotinylated ssDNA tag (50 uM) is added and the solution is incubated at room temperature for 10 minutes with gentle mixing. The beads are then washed and centrifuged another three times and finally suspended in the wash buffer solution. The resulting concentration is 6 mg ml^{-1}.

Assay Protocol

To perform the assay, 10 ul of sFlt-1 at a known concentration in HPLM is diluted with 70 ul of sample diluent (2X PBS, 0.1% BSA, 0.1% Tween 20, 0.1% EDTA). Next, 2.5 ul of antibody functionalized magnetic beads (~1,250,000 beads) are added to the sample and incubated for 2 hours at room temperature with gentle mixing. After 2 hours, the sample is washed to remove any unbound proteins and resuspended in 50 ul of sample diluent along with 1

ul (~786,000 beads) of the dual functionalized polystyrene beads. The sample is incubated for another 2 hours with gentle mixing to allow hybridization. The bead complexes are then separated magnetically and washed seven times with the wash buffer to remove unbound polystyrene beads. After washing, the bead complexes are suspended in 10 ul of 0.1% Tween 20 nuclease-free water and transferred to a 384-well plate for quantification. Real-time qPCR is performed using a BioRad CFX384 Real-Time PCR System. The sample is run alongside a negative control and dilution series of polystyrene beads to produce a standard curve. This protocol is summarized in Figure 5.

Detection

Real-time qPCR is performed using a BioRad CFX384 Real-Time PCR System. Each well contains 10 ul of sample and 15 ul of master mix.

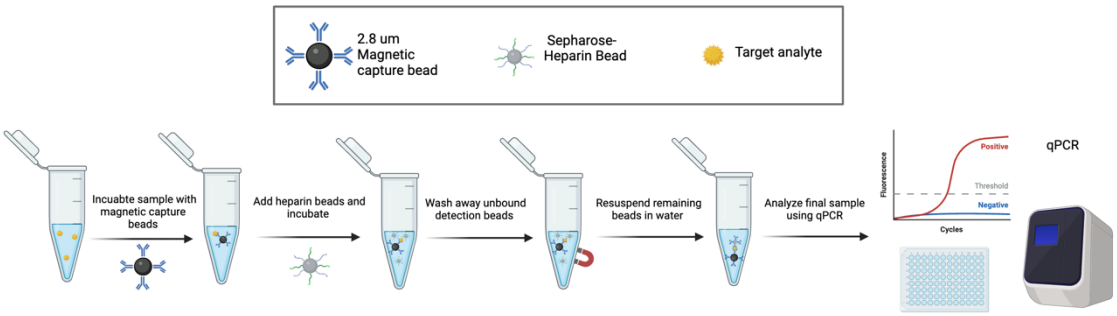

Figure 5. Proposed dual-bead immunoassay. Created with BioRender.com

EXPECTED RESULTS

Due to financial constraints, the preeclampsia assay could not be tested. However, if the assay was run as described, Figure 6 is a representation of an expected result. The red and green blocking represents a pass-fail threshold for the assay, where if the Cq value is within the dynamic range it would signify a sFlt-1 concentration high enough to be flagged as a risk for preeclampsia. Figure 7 shows a sample standard curve that would be produced to quantify experimental results.

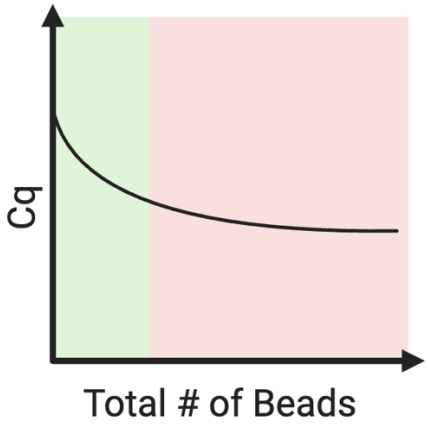

Figure 6. qPCR output showing changes in Cq value. Created with BioRender.com

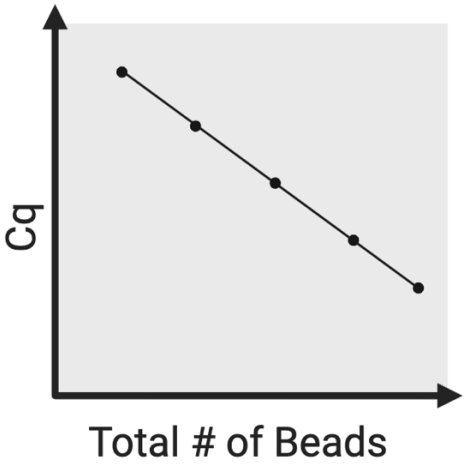

Figure 7. Standard curve. Created with BioRender.com

Chapter 3: Aneuploidy

METHODS

Materials

DNA backbones were purchased from Integrated DNA Technologies. Their sequences are detailed in Table 1. DNA High Sensitivity Reagent Kit was purchased from Revvity for use in the LabChip GX II Touch Nucleic Acid Analyzer. UltraPure™ DNase/RNase-Free Distilled Water, EDTA (0.5 M), pH 8.0, RNase-free, $MgCl_2$ (1 M), S1 Nuclease, and UltraPure™ 1M Tris-HCI, pH 8.0 was purchased from ThermoFisher Scientific for use in sample buffer preparation. Sodium hydroxide was purchased from Sigma-Aldrich for sample buffer preparation. Hydrochloric acid and sodium chloride was purchased from Fisher Scientific for sample buffer preparation.

Table 1. Details for DNA backbones ordered for experiments

Name	Sequence	GC Content (%)	Note
5A	CACAATGATGCACGTTGAAATTAAACCATCTCAAGCCCAATT TACTACTCGTTCTGGTGCTTCTCGTCAGGGCAAGCCTTATTC ACTGAATGAGCAGCTTTGTTACGTTGGTGAAGCGGT	45	model cfDNA with randomized overhang
5B	CAACGTAACAAAGCTGCTCATTCAGTGAATAAGGCTTGCCCT GACGAGAAGCACCAGAACGAGTAGTAAATTGGGCTTGAGA TGGTTTAATTTCAACGTGCATCATTGTG	43.6	model probe
6A	GTTGAAAATCTCCGAACAGCAGGCTCCATAAGCAGCGTTTA ATTACTGGCCTTTATCAGCTTGCTTTCGAGGTGAATTTCTTAA ACAGCTTGATACCGATAGTTGCGCCG	44.5	model probe
6B	CGGCGCAACTATCGGTATCAAGCTGTTTAAGAAATTCACCTC GAAAGCAAGCTGATAAAGGCCAGTAATTAAACGCTGCTTAT GGAGCCTGCTGTTCGGAGATTTTCAACACCGCTTCAC	45.8	model cfDNA with randomized overhang

DNA Preparation

DNA is first diluted 1:100 in the sample buffer used for the experiment. Once diluted, the concentration is measured using The NanoDrop® ND-1000 UV-Vis Spectrophotometer. This value is then used to calculate subsequent dilutions to desired concentrations, as dictated by the experimental protocol.

Hybridization Protocol

The Eppendorf Mastercycler Nexus SX1 was used to hybridize DNA backbones. To hybridize the model probes to the model cfDNA (hybridization 1) and the overhangs to each other (hybridization 2), the thermocycler protocol used is detailed in Table 2.

Table 2. Hybridization Protocol

Step	Time (minutes)	Temperature (°C)
hybridization 1	5	95
	5	85
	5	75
	5	65
	5	55
	5	45
hybridization 2	5	65
	5	55
	5	45
	5	35
	5	25
	hold	12

Hybridization 2 was later changed and the updated protocol in Table 3 was used.

Table 3. Updated Hybridization Protocol

Step	Time (minutes)	Temperature (°C)
hybridization 1	5	95
	5	85
	5	75
	5	65
	5	55
	5	45
hybridization 2 (updated)	20	57
	20	47
	10	37
	5	27
	5	17
	hold	12

This hybridization sequence was used for all experiments except when the order of hybridization was tested.

Experimental Protocol

After the concentration of DNA is determined by the NanoDrop® ND-1000 UV-Vis Spectrophotometer, samples were further diluted to their desired concentrations for a total volume of 80 µl. Complementary backbones were then mixed at a 50/50 ratio and placed in the thermocycler for Hybridization 1, as shown in Table 2 After hybridization, the hybridized backbones are mixed at a 50/50 ratio, unless otherwise specified, and placed in the thermocycler for Hybridization 2 to allow the overhangs to bind. This protocol is summarized in Figure 8. After the second hybridization, the Automated Capillary Electrophoresis Protocol is followed.

Automated Capillary Electrophoresis Protocol

Samples were loaded onto a 96-well plate and transferred onto the LabChip GX II Touch platform. This platform was run with the "HT DNA High Sensitivity" Assay with two sips taken per sample. A custom microfluidic chip was prepared with a gel-dye mixture and DNA markers, provided by Revvity in the DNA High Sensitivity Reagent Kit, and used for analysis. Within the LabChip GX II Touch, a metal sipper on the microfluidic chip is positioned over each sample individually to be analyzed. LabChip GXII Touch is run at 30 ºC. Analysis results in an electropherogram, as represented in Figure 8.

Each prepared plate contained control samples for each DNA backbone and the first hybridization. Samples prepared in buffers with high sodium chloride concentrations were diluted before analysis since sodium chloride effects the performance of the chip and may affect assay sensitivity[38].

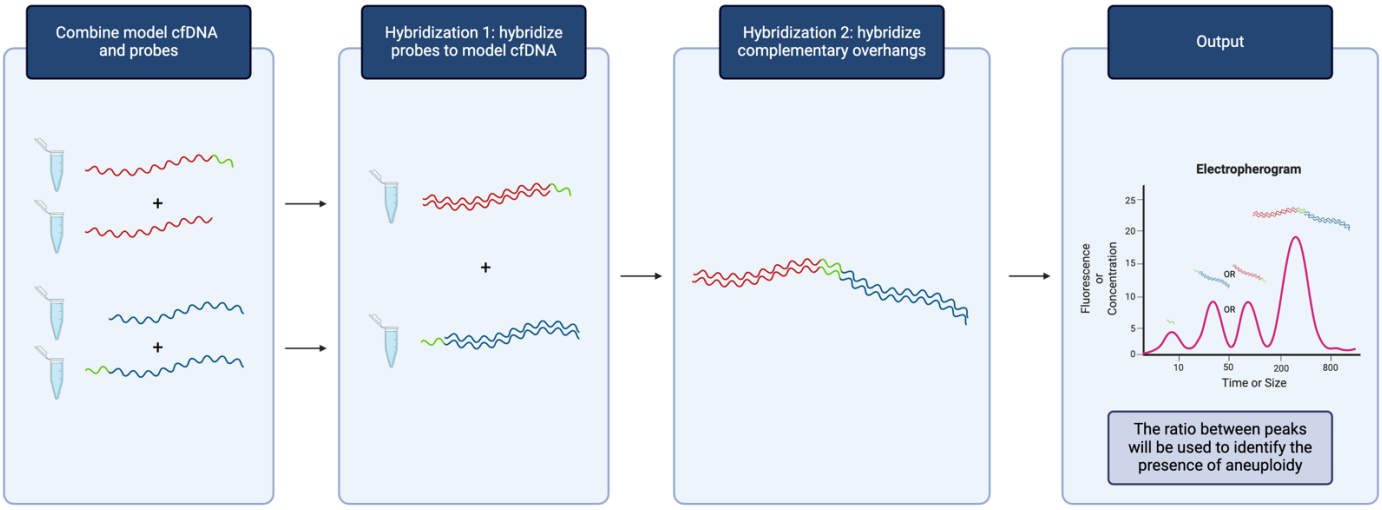

Figure 8. Process flow for sample preparation and expected output. Created with BioRender.com

Hybridization Optimization

In an effort to improve the binding efficiency of the overhangs, concentration of DNA, sample buffer composition, ratio of DNA backbones, and order of hybridization were varied. Changes to the experimental protocol for each of these variations is detailed below. Unless otherwise stated, the hybridization protocol in Table 2 was used for this study.

DNA Concentration

After the concentration of DNA was detected by the NanoDrop® ND-1000 UV-Vis Spectrophotometer, samples were further diluted to concentrations of 0.1µM, 0.25 µM, 0.5 µM, 0.75 µM, and 1 µM. The sample buffer used for analysis was composed of 10 mM TrisHCl, 1 mM EDTA, and 50 mM NaCl. Samples were hybridized following the protocol in Table 2 and then loaded into the LabChip GX II Touch for analysis.

Sample Buffer Composition

It was discovered in the 1960s that hybridization is dependent on salt concentration and is governed by the following equation, where T_m is the melting temperature of DNA, M is the

monovalent cation concentration, and $\%G + C$ is the guanine and cytosine concentration in the sequence[26,27].

$$T_m = 16.6logM + 0.41(\%G + C) + 81.5$$

With this equation in mind, it is understood that ionic strength impacts DNA hybridization and making changes to ion concentrations can impact the hybridization efficiency.

All sample buffers were prepared using UltraPure™ DNase/RNase-Free Distilled Water. Since previous work showed promising results with a higher NaCl concentration of 0.6 M, shown in Figure C - 2, this concentration was used in the sample buffer for subsequent experiments.

Sample buffers with varying concentrations of magnesium chloride ($MgCl_2$) were prepared for analysis. These buffers contained 100 mM, 150 mM, and 200 mM of $MgCl_2$ in addition to 10 mM TrisHCl, 1 mM EDTA, and 0.6 M NaCl. A DNA concentration of 1 μM was used for this study. The updated hybridization protocol in Table 3 was used for this study. Samples were diluted by a factor of 4 and then loaded into the LabChip GX II Touch for analysis.

The pH of the nominal sample buffer containing mM TrisHCl, 1 mM EDTA, and 0.6 M NaCl was found to be about 8. To test the effect of other pHs on hybridization, sample buffers were modified with HCl and NaOH until the desired pHs of 5, 6, 7, and 9 were achieved. pH was monitored using the Mettler-Toledo SevenContact pH/Ion benchtop meter. A DNA concentration of 1 μM was used for this study. The updated hybridization protocol in Table 3 was used for this study. Samples were diluted by a factor of 4 and then loaded into the LabChip GX II Touch for analysis.

To evaluate the effect of sodium dodecyl sulfate (SDS) on hybridization, sample buffer with 10 mM TrisHCl, 1 mM EDTA, 50 mM NaCl, and either 1% (w/v) or 6% (w/v) SDS was used for sample preparation. A DNA concentration of 1 μM was used for this study. The updated hybridization protocol in Table 3 was used for this study. Prior to running the Automated Capillary Electrophoresis protocol, samples were diluted by 10 in nuclease-free water to avoid any potential damage caused by running high concentrations of SDS through the chip.

Ratio of DNA Backbones

Sample buffer with 10 mM TrisHCl, 1 mM EDTA, and 0.6 M NaCl was used for sample preparation. A DNA concentration of 1 μM was used for this study. The ratios of DNA backbones were varied after the first hybridization in preparation for the second hybridization. When the hybridized complementary backbones were combined, four different ratios were used and are listed in Table 4. These ratios were adjusted for a final sample volume of 40 μl. Once combined, samples were placed in the thermocycler for the second hybridization. The hybridization protocol in Table 2 was used. Samples were diluted by a factor of 4 and then loaded into the LabChip GX II Touch for analysis.

Table 4. Ratios of backbones 5 and 6 tested

	% Backbone 5	**% Backbone 6**
Ratio 1	60	40
Ratio 2	40	60
Ratio 3	30	70
Ratio 4	70	30

Order of Hybridization

Sample buffer with 10 mM TrisHCl, 1 mM EDTA, and 0.6 M NaCl was used for sample preparation. A DNA concentration of 0.5 μM was used for this study. Model cfDNA (5A & 6B) were mixed in a 50/50 ratio. Samples were then placed in the thermocycler for the first hybridization. Probes were then added in two ratios, as shown in Table 5. Samples were then

placed in the thermocycler for the second hybridization. The updated hybridization protocol in Table 3 was used for this study. Samples were diluted by a factor of 4 and then loaded into the LabChip GX II Touch for analysis.

Table 5. Sample preparation for hybridization 2 by volume in microliters

	5A+6B	**5B**	**6A**
Group 1	20	10	10
Group 2	20	20	20

Excess of Probes

Sample buffer with 10 mM TrisHCl, 1 mM EDTA, and 0.6 M NaCl was used for sample preparation. A DNA concentration of 1 μM was used for this study. Since in the Vanadis workflow an excess of probes will be added to samples, an excess of probes in the model DNA was tested. Probes were added in 10x excess prior to the first hybridization. The hybridization protocol in Table 2 was used. Results were compared against a control without excess probes. Samples were diluted by a factor of 4 and then loaded into the LabChip GX II Touch for analysis.

Nuclease Cleanup

The 'Excess of Probes' protocol was followed with nuclease added after the second hybridization. By adding nuclease to the samples, the excess probe will in theory break down and result in clearer peaks for analysis. Nuclease was prepared in a 1:100 dilution. Reaction buffer with 10 mM $MgCl_2$, 10 mM TrisHCl, 1 mM EDTA, and 0.6 M NaCl was used. Samples were incubated for 30 minutes at room temperature. Following incubation, 2 μl of EDTA was added and samples were incubated at 70°C for 10 minutes in the thermocycler. Samples were diluted by a factor of 4 and then loaded into the LabChip GX II Touch according to the Automated Capillary Electrophoresis protocol.

Data Analysis

A custom MATLAB script, found in Appendix B, was used to calculate the area under the curve and peak height for analysis. A ratio between the area under the curve was used to evaluate normalized DNA hybridization.

Statistical Analysis

Statistical tests were performed using GraphPad Prism 10.1.1. Unless otherwise noted, a repeated measures ANOVA with post-hoc Tukey test was performed.

RESULTS & DISCUSSION

DNA Concentration

DNA concentration was varied to assess the effect of concentration on hybridization efficiency. At low concentrations (0.1 and 0.25 μM), only one out of the two technical replicates produced results that could be analyzed using the custom MATLAB code. A repeated measures ANOVA was used to assess statistical significance between groups that had two technical replicates (0.5, 0.75, 1 μM) while a one-way ANOVA was used to assess the remaining groups. No statistically significant differences were found. Since there was no significant difference between the conditions, 1 μM was used for subsequent experiments unless otherwise noted.

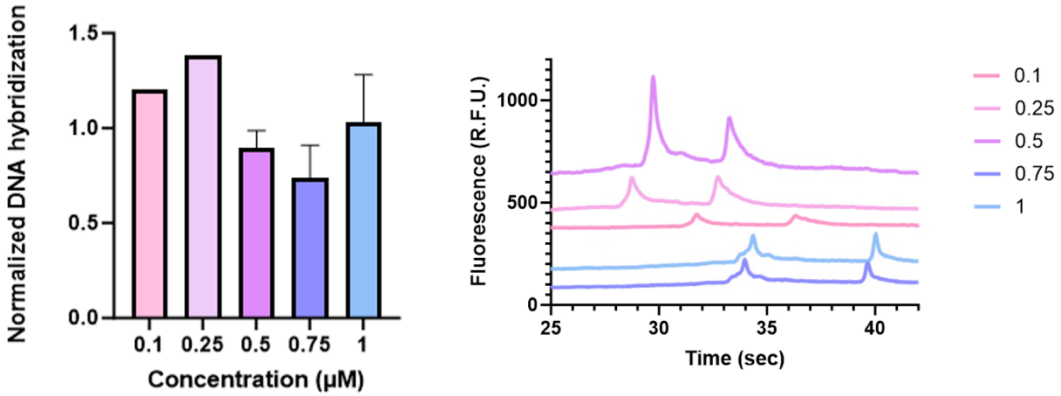

Figure 9. Effect of DNA concentration on normalized DNA hybridization where error bars reflect technical replicates (n=2) (left) and representative electropherogram of samples with varying DNA concentration (right). Electropherogram shows relative fluorescence, as

fluorescence values were shifted to present all data groups. 0.1 & 0.25 μM were also shifted by -5 seconds to best fit on graph.

Concentration had little effect on normalized DNA hybridization, as shown in Figure 9. Some results produced were unable to be analyzed further, namely one of each technical replicate for the lower concentration samples. This may be because of damage to the chip or issues with assay setup. Troubleshooting LabChip GX II Touch resolved these issues, but the outcome of this experiment was selecting 1 μM for future experiments. 1 μM was selected since the next experiments would be using high salt buffers that needed to be diluted before sample analysis. By using the maximum concentration tested, the fluorescent signal could still be easily analyzed despite the dilutions.

Sample Buffer Composition

Studies reported the benefits of $MgCl_2$ in hybridization events, like their potential to stabilize DNA duplexes[28,29]. Since cations bind to nucleic acids, a shielding effect against the negatively charged backbone occurs, causing magnesium to stabilize DNA duplexes through this interaction and facilitate folding into biologically active structures[28,29]. Because of this stabilization, it was theorized that preparing sample buffer with $MgCl_2$ could enhance hybridization. Low concentrations of $MgCl_2$ were previously explored but yielded inconclusive results, therefore higher concentrations were tested in this experiment. Three concentrations were prepared: 100, 150, and 200 mM. Results are shown in Figure 10.

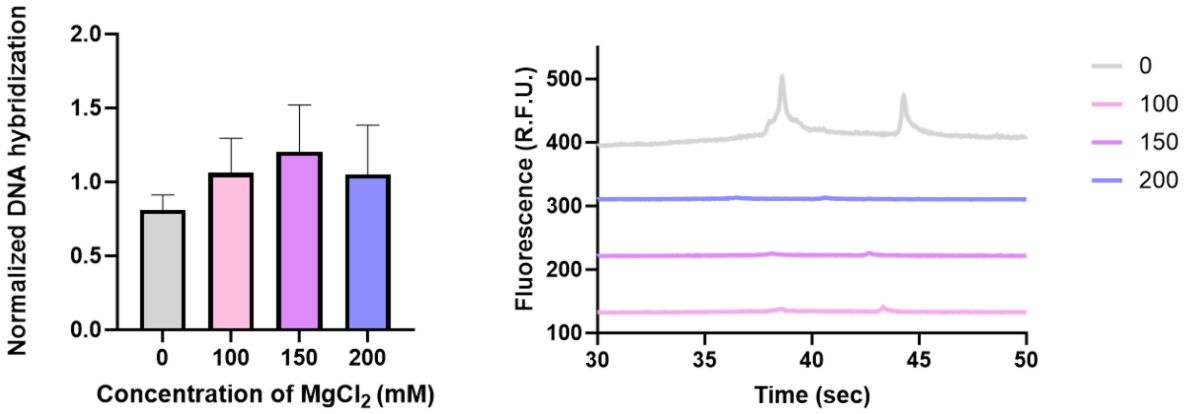

Figure 10. Effect of $MgCl_2$ at varying concentrations on normalized DNA hybridization where error bars reflect technical replicates (n=2) (left) and representative electropherogram of samples with varying $MgCl_2$ concentration (right). Electropherogram shows relative fluorescence, as fluorescence values were shifted to present all data groups.

Although there appears to be a marginal improvement in hybridization, it was not statistically significant according to the results of the repeated measures ANOVA. The addition of $MgCl_2$ also subdued the fluorescent signal, making analysis more difficult. Because of this, it was excluded from sample preparation for subsequent experiments and it is not recommended to use $MgCl_2$ in sample buffer moving forward.

pH was identified as an important factor in hybridization optimization in previous studies. pHs of 5-9 were explored, where pH of 8 was identified as the nominal pH for the sample buffer used in previous experiments. A pH of 6 showed the greatest improvement in hybridization, so this was selected as the optimal pH for sample preparation and is recommended for future work. A repeated measures ANOVA was performed and found statistical significance between pH 7 and 8 ($p=0.0211$).

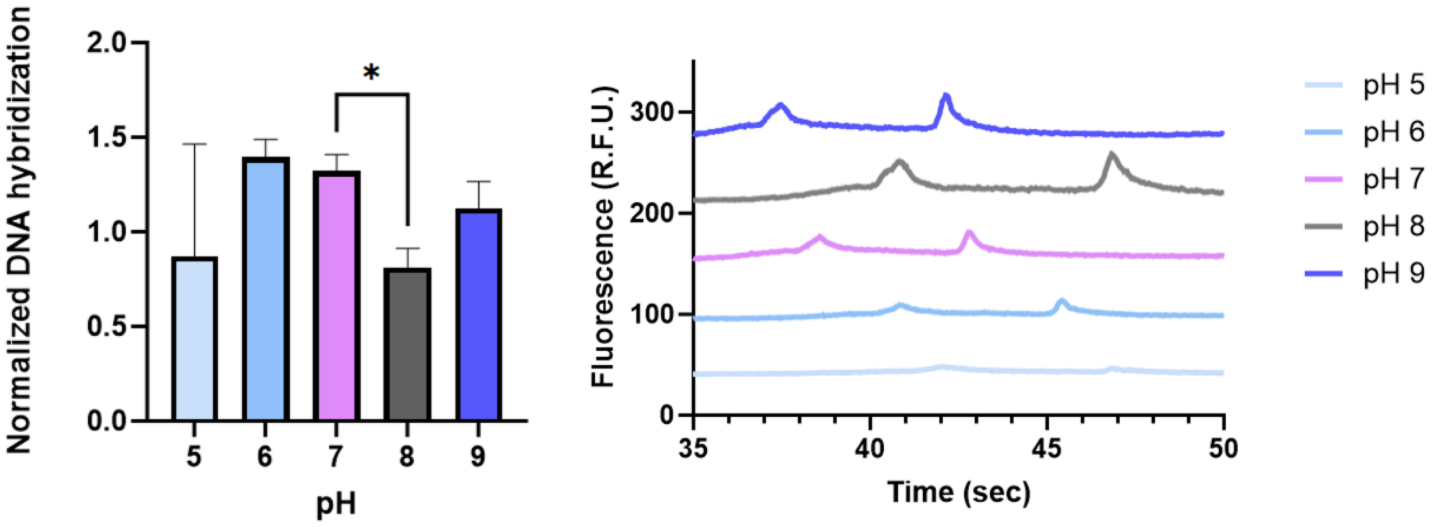

Figure 11. Effect of pH on normalized DNA hybridization where pH 8 is the control and where error bars reflect technical replicates (n=2) (left) and representative electropherogram of samples with varying pH (right). Electropherogram shows relative fluorescence, as fluorescence values were shifted to present all data groups.

The effect of pH on hybridization has been well documented in the literature[30]. Changes in pH can affect the protonation of nucleic acids, disrupting hydrogen bonds and ultimately affecting DNA backbone stability. Earlier studies theorized lower pHs, which protonated nucleic acids, exhibited a comparable stabilizing effect as ionic salts by shielding the negative charge of the phosphate group and reducing electrostatic interactions, while the opposite effect occurs at higher pHs. These studies found hybridization rates were optimal between a pH of 5 and 9[30]. To identify the optimal pH for hybridization in this study, sample buffers with a pH range of 5-9 were prepared and tested. Results demonstrate a pH of 6 produced the highest normalized DNA hybridization, as shown in Figure 11, however this result was not statistically significant. Although pH 6 had a higher normalized DNA hybridization, it was not statistically different from the other pHs tested. The standard errors of the difference between the means were too high to result in a p-value <0.05. However, there were only two technical replicates performed, so this

may be an artifact of a small sample size. A pH of 6 has been identified as the optimal pH for future work, however because of its statistical insignificance, this study should be repeated with a higher sample size to verify. Slightly acidic/near neutral pH may have been best for hybridization because these pH values are not far from the pK_a of nucleic acid bases[30].

Some studies showed greater hybridization efficiency with buffers that contained SDS[27]. However, the use of SDS in microfluidics carries a risk of damaging the chip since SDS produces microbubbles[31]. To mitigate this risk, samples were prepared and hybridized in low concentrations of SDS (1% and 6%, w/v) and diluted 10-fold in nuclease-free water prior to analysis. Results, shown in Figure 12, show a significant decrease in DNA hybridization and relative fluorescence with samples prepared with SDS. This could be due to the effect SDS has on the dissociation temperature, meaning with the addition of SDS, the hybridization temperatures used may need to be increased to see effective hybridization.

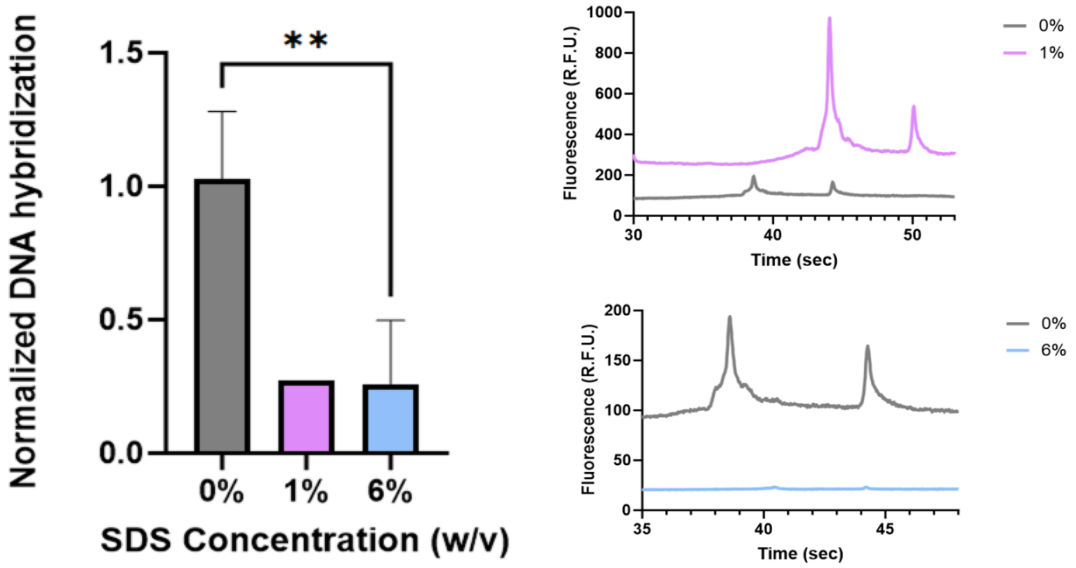

Figure 12. Effect of SDS concentration on normalized DNA hybridization compared to a control without SDS where error bars reflect technical replicates (n=2) (left) and representative electropherogram of samples with varying SDS concentration (right). Electropherogram shows relative fluorescence, as fluorescence values were shifted to present all data groups.

SDS showed a significant decrease in normalized DNA hybridization, in addition to reducing the fluorescent signal and making analysis more difficult. Since only one technical replicate in the 1% group could be analyzed, a repeated measures ANOVA could not be used for statistical assessment. A paired t-test revealed a statistically significant difference between the 6% group and the control ($p=0.0070$). An unpaired t-test was used to assess statistics for the 1% group against the control and 6% group and found no significance. Using SDS for sample preparation introduces the risk of damaging the chip because of the microbubbles it produces. Because of these complications and results, SDS is not recommended for sample preparation.

Ratio of DNA Backbones

The ratio of DNA backbones was varied after the first hybridization. Results showed that a ratio of 50/50 or 60/40 produces the highest normalized DNA hybridization. A repeated measures ANOVA revealed a statistically significant difference between Ratio 1 (60/40) and Ratio 2 (40/60) with a p-value of 0.0347. To keep the workflow simple, 50/50 is recommended for subsequent experiments.

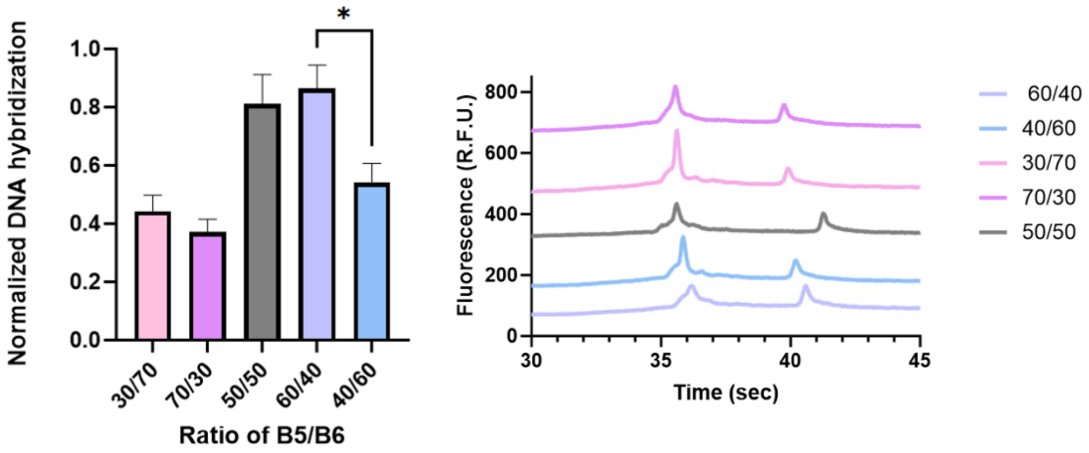

Figure 13. Effect of backbone ratio on normalized DNA hybridization where error bars reflect technical replicates (n=2) (left) and representative electropherogram of samples with varying backbone ratios (right). Electropherogram shows relative fluorescence, as fluorescence

values were shifted to present all data groups. Time for the control group (50/50) was also shifted by -3 seconds to best fit on the graph.

Previous work done by the team explored measuring DNA concentration using Qubit compared to the NanoDrop and found a discrepancy, shown in Figure C - 3. Since desired concentration was achieved using the measured concentration from NanoDrop, any measurement errors from the NanoDrop could largely impact the ratio of model cfDNA to probes and ultimately the ratio of backbones produced during the experimental protocol. To explore if this was possibly occurring and also mitigate any potential discrepancy, an experiment was performed in which the ratios of backbones combined prior to the second hybridization was varied. As shown in Figure 13, a ratio of 60/40 is comparable to the control, while ratios of 30/70, 70/30, and 40/60 showed decreased efficiency. This suggests the actual concentrations for backbone 5 may be slightly lower than measured and the actual concentrations for backbone 6 may be slightly higher than measured. Since it was close to the control and did not show a significant difference in normalized DNA hybridization, it was not flagged as a concern at this time and was assumed that the actual concentration was approximately equal to the measured concentration. If a greater discrepancy was shown or there was a statistically significant increase in normalized DNA hybridization, an alternative manufacturer of DNA could be used or an alternative method for measuring DNA concentration could be explored.

Order of Hybridization

After exploring changes in sample buffer, it was theorized that the conformation of DNA may be hindering hybridization. Since DNA is negatively charged, electrostatic effects may have been preventing the overhangs from binding. To explore this, the order of hybridization was changed, where model cfDNA was combined and hybridized first, then the probes were added and hybridized to model cfDNA. A repeated measures ANOVA showed no statistically

significant difference between groups. The standard hybridization order was used for subsequent experiments.

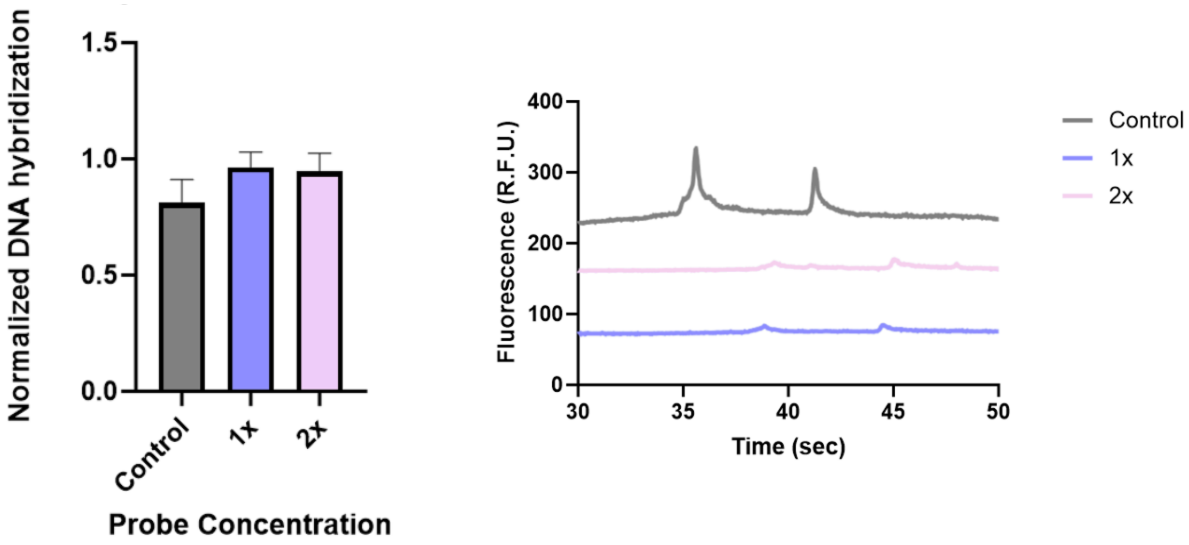

Figure 14. Effect of hybridization order on normalized DNA hybridization with different probe concentrations tested where error bars reflect technical replicates (n=2). (left). The control results are pulled from another experiment with the standard hybridization order as described previously and a DNA concentration of 1 μM. Representative electropherogram of samples with varying probe concentration against a control (right). Electropherogram shows relative fluorescence, as fluorescence values were shifted to present all data groups.

As shown in Figure 14, there was no difference in normalized DNA hybridization. Although this didn't confirm nor deny the theory, it did confirm the significance of the second hybridization and the need to further optimize the hybridization of the overhangs.

Excess of Probes & Nuclease Cleanup

Since the workflow of this assay in a clinical setting would require the probes to be in excess, this was simulated experimentally by adding ten times the volume of probes for the first hybridization. Results showed an improvement in nominal DNA hybridization. A repeated measures ANOVA showed no statistically significant difference between groups. A nuclease cleanup step was explored to remove excess probes and streamline analysis, but because the

workflow to activate the nuclease required heating it to 70 °C, an unexpected result was the breakdown of the hybridized product. This drastically decreased the normalized DNA hybridization.

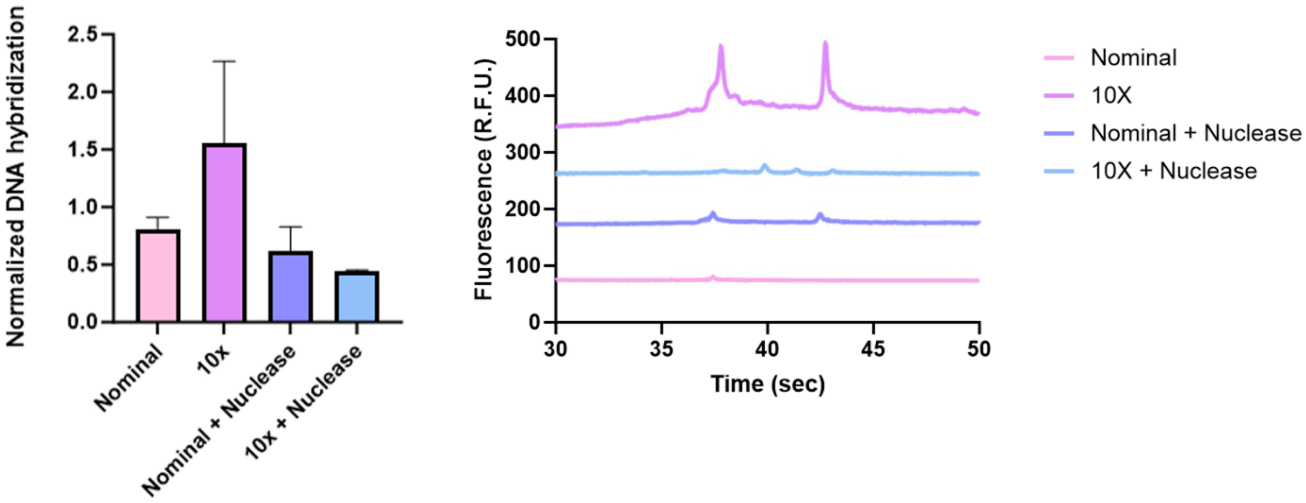

Figure 15. Effect of an excess of probes and nuclease clean up step on normalized DNA hybridization where error bars reflect technical replicates (n=2) (left) and representative electropherogram of samples with and without an excess of probes and nuclease (right). Electropherogram shows relative fluorescence, as fluorescence values were shifted to present all data groups.

Results, shown in Figure 15, are as expected, where compared to the control, there is a much higher normalized DNA hybridization with excess probes. However, excess probes can show up as an additional peak in the electropherogram, complicating analysis. Nuclease was introduced as a potential solution, where the non-specific DNA-ase could cleave any single stranded DNA immediately prior to analysis. However, $MgCl_2$ was used to prepare the nuclease instead of zinc sulfate, so the reaction buffer was not ideal. Nuclease additionally required a heating step to take effect, but the incubation temperature used was above the T_m of DNA. These preparation issues caused two things: first, excess probe did not break down as expected, since

the reaction buffer was prepared incorrectly, and second, the high incubation temperature caused the hybridized DNA to breakdown.

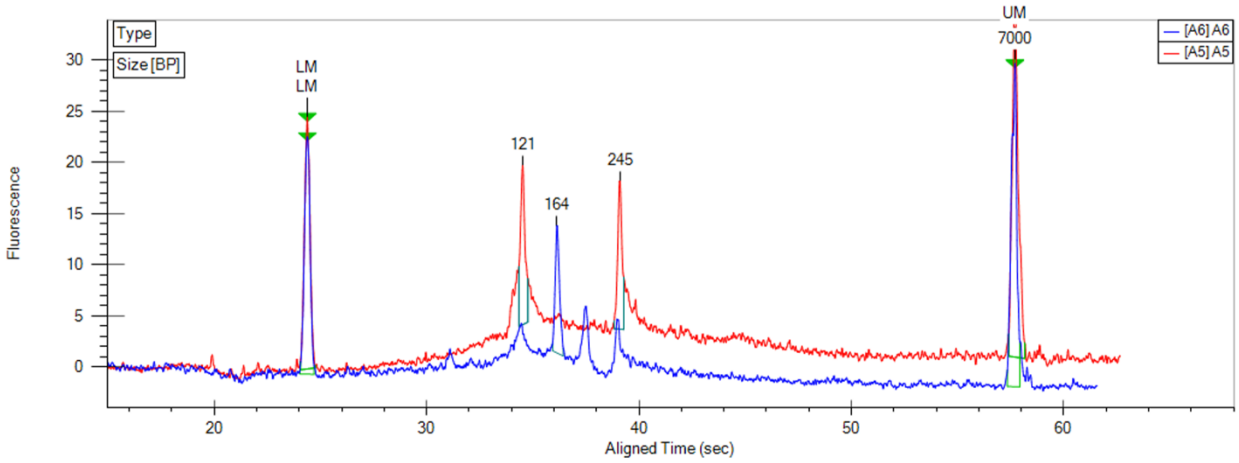

Figure 16. Electropherogram for hybridized DNA with excess probes and nuclease where the red line represents the control and the blue represents an excess of probes with nuclease added.

Figure 16 shows an overlayed electropherogram where the blue line is the sample prepared with excess probe and nuclease and the red line is the control. The peaks representing the hybridized backbones and fully hybridized product line up and the excess probe peaks rest in between them, demonstrating that the nuclease was ineffective in breaking down excess probes in this experiment. A nuclease clean-up step can be explored again in the future, but care should be taken to prepare in the appropriate reaction buffer and adjust the incubation temperature.

Chapter 4: Conclusions

Since the preeclampsia project could not be executed further in the course of this thesis, future work can focus on further developing the idea and executing it as detailed here.

For the aneuploidy project, there are a variety of different approaches that can be taken to further optimize hybridization. The maximum normalized DNA hybridization achieved in this thesis was 1.43. Achieving a normalized DNA hybridization of 1.5 or greater would allow for a more robust and sensitive assay. Some simple changes that can be implemented are adding a control that is the same length and weight as the fully hybridized product to compare to on the electropherogram. In the experiments performed in this study, a control ladder was used to quantify peak size and migration. Individual backbones and hybridized backbones were included in each run as a control and used during analysis of the fully hybridized product to troubleshoot and identify extraneous peaks present. Having a similar control that is of equal size and weight to the fully hybridized product could help identify and troubleshoot any issues with future experiments. Another change that can be made to the workflow is the addition of a ligation step, using a ligase, such as T3, T4, or T7 ligase, that binds to phosphate groups after the second hybridization[33]. This would eliminate the electrostatic interactions caused by the unbound phosphate groups and could enhance hybridization.

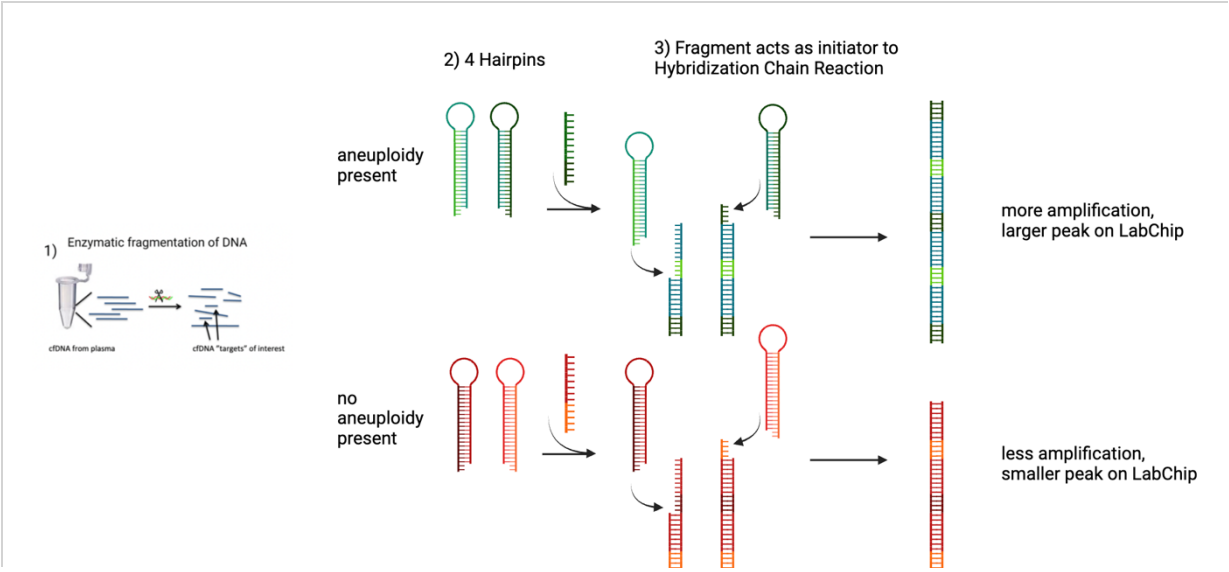

Figure 17. Alternative approach for hybridization and amplification. Created with Biorender.com

An alternative approach that could be explored in the future is the use of hairpin DNA for DNA amplification through a hybridization chain reaction. In this process, shown in Figure 17, two sets of DNA hairpin molecules are used along with an initiator strand of DNA to trigger a chain reaction of hybridization events. This process allows for amplification without the need for PCR. For NIPT, the initiator strand would be the cfDNA fragments. If aneuploidy is present, the resulting product would be significantly longer than non-aneuploid fragments. In this workflow, aneuploidy can still be detected without quantitative analysis[34-36].

An alternative to the randomized overhang could be a photo crosslinker, where instead of relying on a second hybridization event to initiate binding of the overhangs, binding could be carefully controlled through a photochemical reaction[37]. In this workflow, cfDNA is modified with a photo crosslinker instead of a randomized overhang, linearized DNA would bind to probes during the first hybridization, and a photochemical reaction would bind the crosslinkers. This could result in a more controlled binding reaction.

Lower concentrations of DNA can also be explored in future work. Although concentrations of 0.1 μM were explored in this thesis, some studies report successful DNA hybridization at the nanomolar scale[32]. Since there are two hybridization steps in this workflow, there may be an overcrowding effect as DNA is replicated. Using a lower starting concentration may mitigate this effect, resulting in better secondary hybridization, and therefore should be explored in subsequent studies.

The work described in this thesis introduces two novel methods in perinatal health screening. A novel dual-bead assay was presented as a method to screen for preeclampsia. Although this work was not completed in the course of this thesis, the methods can be used in future work to develop the concept and produce a robust screening test. A novel way to screen for aneuploidy using automated capillary electrophoresis and nonquantitative analysis was also presented. After a series of experiments were performed to optimize the hybridization efficiency of the overhangs in this test, optimal conditions were identified and future work laid out to further optimize this method. The changes to the NIPT workflow for aneuploidy open an opportunity for a high throughput, fast, and non-quantitative test to be used as a screening test for aneuploidies of chromosome 18 and 21. This work can be expanded to other chromosomes and potentially multiplexed in the future, to provide a robust, singular test to screen all the most common aneuploidies.

References

1. Ahmad, A. (2023, May 14). America has the highest maternal mortality rate among developed nations–and it's on the rise. here's why we are facing a pregnancy health crisis. Fortune. https://fortune.com/2023/05/14/america-highest-maternal-mortality-rate-among-developed-nationsand-rise-pregnancy-health-crisis-asima-ahmad/
2. The White House. (2022, April 13). *Fact sheet: Biden-Harris Administration announces additional actions in response to vice president Harris's call to action on maternal health*. https://www.whitehouse.gov/briefing-room/statements-releases/2022/04/13/fact-sheet-biden-harris-administration-announces-additional-actions-in-response-to-vice-president-harriss-call-to-action-on-maternal-health/
3. Katella, K. (2023, May 22). *Maternal mortality is on the rise: 8 things to know*. Yale Medicine. https://www.yalemedicine.org/news/maternal-mortality-on-the-rise
4. *Prenatal tests*. March of Dimes. (2020, September). https://www.marchofdimes.org/find-support/topics/planning-baby/prenatal-tests
5. Ford, N. D., Cox, S., & Ko, J. Y. (2022, April 28). Hypertensive disorders in pregnancy and mortality at delivery hospitalization - United States, 2017–2019. Centers for Disease Control and Prevention. https://www.cdc.gov/mmwr/volumes/71/wr/mm7117a1.htm?s_cid=mm7117a1_w
6. Ogunyemi, D. (2022, January). 3 conditions to watch for after childbirth. ACOG. https://www.acog.org/womens-health/experts-and-stories/the-latest/3-conditions-to-watch-for-after-childbirth#:~:text=Postpartum%20preeclampsia%20most%20often%20happens,seizures%2C%20and%20other%20serious%20problems
7. Karrar SA, Hong PL. Preeclampsia. [Updated 2023 Feb 13]. In: StatPearls [Internet]. Treasure Island (FL): StatPearls Publishing; 2023 Jan-. Available from: https://www.ncbi.nlm.nih.gov/books/NBK570611/
8. Shimkhada, R., Solon, O., Tamondong-Lachica, D., & Peabody, J. W. (2016). Misdiagnosis of obstetrical cases and the clinical and cost consequences to patients: a cross-sectional study of urban providers in the Philippines. Global health action, 9, 32672. https://doi.org/10.3402/gha.v9.32672
9. Wang Y, Zhao S. Vascular Biology of the Placenta. San Rafael (CA): Morgan & Claypool Life Sciences; 2010. Chapter 2, Placental Blood Circulation. Available from: https://www.ncbi.nlm.nih.gov/books/NBK53254/
10. Staff, A. C., Fjeldstad, H. E., Fosheim, I. K., Moe, K., Turowski, G., Johnsen, G. M., Alnaes-Katjavivi, P., & Sugulle, M. (2022). Failure of physiological transformation and spiral artery atherosis: their roles in preeclampsia. American journal of obstetrics and gynecology, 226(2S), S895–S906. https://doi.org/10.1016/j.ajog.2020.09.026
11. Margioula-Siarkou, G., Margioula-Siarkou, C., Petousis, S., Margaritis, K., Vavoulidis, E., Gullo, G., Alexandratou, M., Dinas, K., Sotiriadis, A., & Mavromatidis, G. (2022). The role of endoglin and its soluble form in pathogenesis of preeclampsia. Molecular and cellular biochemistry, 477(2), 479–491. https://doi.org/10.1007/s11010-021-04294-z
12. Palmer, K. R., Tong, S., & Kaitu'u-Lino, T. J. (2017). Placental-specific sFLT-1: role in pre-eclamptic pathophysiology and its translational possibilities for clinical prediction and diagnosis. Molecular human reproduction, 23(2), 69–78. https://doi.org/10.1093/molehr/gaw077

13. Chau, K., Hennessy, A., & Makris, A. (2017). Placental growth factor and pre-eclampsia. Journal of human hypertension, 31(12), 782–786. https://doi.org/10.1038/jhh.2017.61
14. Maynard, S. E., Min, J. Y., Merchan, J., Lim, K. H., Li, J., Mondal, S., Libermann, T. A., Morgan, J. P., Sellke, F. W., Stillman, I. E., Epstein, F. H., Sukhatme, V. P., & Karumanchi, S. A. (2003). Excess placental soluble fms-like tyrosine kinase 1 (sFlt1) may contribute to endothelial dysfunction, hypertension, and proteinuria in preeclampsia. The Journal of clinical investigation, 111(5), 649–658. https://doi.org/10.1172/JCI17189
15. Shibuya, M., Matsui, H., Sasagawa, T., & Nagamatsu, T. (2021). A simple detection method for the serum sFLT1 protein in preeclampsia. Scientific reports, 11(1), 20613. https://doi.org/10.1038/s41598-021-00152-6
16. Jia, C. W., Wang, L., Lan, Y. L., Song, R., Zhou, L. Y., Yu, L., Yang, Y., Liang, Y., Li, Y., Ma, Y. M., & Wang, S. Y. (2015). Aneuploidy in Early Miscarriage and its Related Factors. Chinese medical journal, 128(20), 2772–2776. https://doi.org/10.4103/0366-6999.167352
17. Griffin D. K. (1996). The incidence, origin, and etiology of aneuploidy. *International review of cytology*, *167*, 263–296. https://doi.org/10.1016/s0074-7696(08)61349-2
18. Bonus, M. L., McQueen, D. B., Ruderman, R., Hughes, L., Merrion, K., Maisenbacher, M. K., Feinberg, E., & Boots, C. (2022). Relationship between paternal factors and embryonic aneuploidy of paternal origin. *Fertility and sterility*, *118*(2), 281–288. https://doi.org/10.1016/j.fertnstert.2022.04.020
19. Cserhati M. (2021). Calculation of Fetal Fraction for Non-Invasive Prenatal Testing. Biotech (Basel (Switzerland)), 10(3), 17. https://doi.org/10.3390/biotech10030017
20. Nagaoka, S. I., Hassold, T. J., & Hunt, P. A. (2012). Human aneuploidy: mechanisms and new insights into an age-old problem. Nature reviews. Genetics, 13(7), 493–504. https://doi.org/10.1038/nrg3245
21. Gregg, A. R., Skotko, B. G., Benkendorf, J. L., Monaghan, K. G., Bajaj, K., Best, R. G., Klugman, S., & Watson, M. S. (2016). Noninvasive prenatal screening for fetal aneuploidy, 2016 update: a position statement of the American College of Medical Genetics and Genomics. Genetics in medicine : official journal of the American College of Medical Genetics, 18(10), 1056–1065. https://doi.org/10.1038/gim.2016.97
22. Alberry, M. S., Aziz, E., Ahmed, S. R., & Abdel-Fattah, S. (2021). Non invasive prenatal testing (NIPT) for common aneuploidies and beyond. European journal of obstetrics, gynecology, and reproductive biology, 258, 424–429. https://doi.org/10.1016/j.ejogrb.2021.01.008
23. Dahl, F., Ericsson, O., Karlberg, O., Karlsson, F., Howell, M., Persson, F., Roos, F., Stenberg, J., Ahola, T., Alftrén, I., Andersson, B., Barkenäs, E., Brandner, B., Dahlberg, J., Elfman, S., Eriksson, M., Forsgren, P. O., Francois, N., Gousseva, A., Hakamali, F., … Nicolaides, K. (2018). Imaging single DNA molecules for high precision NIPT. Scientific reports, 8(1), 4549. https://doi.org/10.1038/s41598-018-22606-0
24. Coll De Peña, A. (2024). Characterization of Nucleic Acid Delivery Vehicle Products using Microfluidic Concepts. [Doctoral thesis, Brown University].
25. James, N. (2011). Chapter 4: Capillary Electrophoresis. In GAS CHROMATOGRAPHY, LIQUID CHROMATOGRAPHY, CAPILLARY ELECTROPHORESIS - MASS SPECTROMETRY: A BASIC INTRODUCTION. Whitman College. Retrieved April 10, 2024, from http://people.whitman.edu/~dunnivfm/C_MS_Ebook/Prelim/index.html.
26. Schildkraut C. (1965). Dependence of the melting temperature of DNA on salt concentration. Biopolymers, 3(2), 195–208. https://doi.org/10.1002/bip.360030207

27. Rose, K., Mason, J. O., & Lathe, R. (2002). Hybridization parameters revisited: solutions containing SDS. BioTechniques, 33(1), 54–58. https://doi.org/10.2144/02331st01
28. Springer, T., Sípová, H., Vaisocherová, H., Stepánek, J., & Homola, J. (2010). Shielding effect of monovalent and divalent cations on solid-phase DNA hybridization: surface plasmon resonance biosensor study. Nucleic acids research, 38(20), 7343–7351. https://doi.org/10.1093/nar/gkq577
29. Owczarzy, R., Moreira, B. G., You, Y., Behlke, M. A., & Walder, J. A. (2008). Predicting stability of DNA duplexes in solutions containing magnesium and monovalent cations. Biochemistry, 47(19), 5336–5353. https://doi.org/10.1021/bi702363u
30. Wong, K. L., & Liu, J. (2021). Factors and methods to modulate DNA hybridization kinetics. Biotechnology journal, 16(11), e2000338. https://doi.org/10.1002/biot.202000338
31. Deng, B., Schroën, K., & de Ruiter, J. (2023). A microfluidic study of bubble formation and coalescence tuned by dynamic adsorption of SDS and proteins. *Food Hydrocolloids*, *140*, 108663. https://doi.org/10.1016/J.FOODHYD.2023.108663
32. Markegard, C. B., Gallivan, C. P., Cheng, D. D., & Nguyen, H. D. (2016). Effects of Concentration and Temperature on DNA Hybridization by Two Closely Related Sequences via Large-Scale Coarse-Grained Simulations. The journal of physical chemistry. B, 120(32), 7795–7806. https://doi.org/10.1021/acs.jpcb.6b03937
33. Biolabs, N. E. (2024). DNA Ligase Selection Chart. NEB. https://www.neb.com/en-us/tools-and-resources/selection-charts/dna-ligase-selection-chart
34. Xu, G., Lai, M., Wilson, R. et al. Branched hybridization chain reaction—using highly dimensional DNA nanostructures for label-free, reagent-less, multiplexed molecular diagnostics. Microsyst Nanoeng 5, 37 (2019). https://doi.org/10.1038/s41378-019-0076-z
35. Dirks, R. M., & Pierce, N. A. (2004). Triggered amplification by hybridization chain reaction. Proceedings of the National Academy of Sciences of the United States of America, 101(43), 15275–15278. https://doi.org/10.1073/pnas.0407024101
36. P. V. Riccelli, F. Merante, K. T. Leung, S. Bortolin, R. L. Zastawny, R. Janeczko, Albert S. Benight, Hybridization of single-stranded DNA targets to immobilized complementary DNA probes: comparison of hairpin versus linear capture probes, Nucleic Acids Research, Volume 29, Issue 4, 15 February 2001, Pages 996–1004, https://doi.org/10.1093/nar/29.4.996
37. Chen, C., & Peng, T. (2020). Protocol for Site-Specific Photo-Crosslinking Proteomics to Identify Protein-Protein Interactions in Mammalian Cells. STAR protocols, 1(3), 100109. https://doi.org/10.1016/j.xpro.2020.100109
38. PerkinElmer. (2014-2016). DNA High Sensitivity Assay User Guide For LabChip GX Touch/GXII Touch. https://resources.perkinelmer.com/lab-solutions/resources/docs/gde_dna-high-sens-user-guide.pdf

Appendix A. LabChip GX II Touch Specifications

The below tables are adapted from Revvity's DNA High Sensitivity Assay User Guide[38].

Table A - 1. Assay specifications. Adapted from Revvity's Assay User Guide.

Sizing Range	50 - 5000 bp
Sizing Resolution	± 5% from 100 - 500 bp ± 10% from 50 - 100 bp, 500 - 1000 bp ± 15% from 1000 - 3000 bp ± 22% from 3000 - 5000 bp
Sizing Accuracy	± 10%
Sizing Precision	5% CV
Linear Concentration Range	**Standard Sample Workflow** 10 pg/µL - 500 pg/µL per fragment from 50 bp to 2000 bp 50 pg/µL - 500 pg/µL per fragment from 2000 bp to 5000 bp 100 pg/µL - 5 ng/µL for smears **Limited Sample Workflow (initial concentration)** 20 pg/µL - 500 pg/µL per fragment from 50 bp to 2000 bp 100 pg/µL - 500 pg/µL per fragment from 2000 bp to 5000 bp 200 pg/µL - 5 ng/µL for smears
	Standard Workflow 5 pg/µL per fragment 100 pg/µL for smears **Limited Sample Workflow (initial concentration)** 10 pg/µL per fragment 200 pg/µL for smears
Maximum Total DNA Concentration	5 ng/µL total, 500 pg/µL per fragment
Quantitation Accuracy	± 30%
Sizing Range	50 – 5000 bp
Quantitation Precision	20% CV
Analysis Time	68 seconds per sample (~2.5 hours for 96 samples)
Number of Samples per Chip Prep	96 samples

Table A - 2. Sample Conditions. Adapted from Revvity's Assay User Guide.

Additives	Revvity recommends that BSA and detergents exceeding 0.05 mg/mL and 0.01% (v/v) respectively in concentration not be used. Higher concentrations can result in chip failure. In addition, nonaqueous solvents are not compatible with DNA LabChip protocols.
Particulates	All sample plates should be spun down prior to analysis. All buffers should be

	filtered with a 0.22 µm cellulose acetate filter.
Salt Concentration	Total salt concentration must not exceed 10 mM Tris and 1 mM EDTA for the DNA High Sensitivity assay. Higher salt concentrations and different ions may alter performance and reduce assay sensitivity.

Appendix B. Custom MATLAB Script

Created by Allistair Yu

```
M = readmatrix('FILE_NAME.csv');

x = M(:,1);
y = M(:,12); % choose which column/sample you want to analyze

plot(x,y);

while 1
    try
        [x_coord, y_coord] = ginput(2);
    catch
        fprintf("figure deleted\n");
        break;
    end
    if x_coord ~= sort(x_coord)
        x_coord = sort(x_coord);
        temp = y_coord(2);
        y_coord(2) = y_coord(1);
        y_coord(1) = temp;
    end

    % get closest start and end x values
    [val, start_idx] = min(abs(x-x_coord(1)));
    x_start = x(start_idx);
    y_start = y(start_idx);
    [val, end_idx] = min(abs(x-x_coord(2)));
    x_end = x(end_idx);
    y_end = y(end_idx);

    % get subset of data based on range
    x_sub = x(start_idx:end_idx);
    y_sub = y(start_idx:end_idx);

    % calculate peak height in range
    peak_height = max(y(start_idx:end_idx));

    % calculate fwhmx
    % get height of peak using y-value at start of peak
    % can easily change to be dynamic so that it gets larger height value
    % instead of always using start of peak
    height = peak_height - y(start_idx); % can change to
min(y(start_idx),y(end_idx))
    half_max = height / 2 + y(start_idx);
    disp(half_max);
    half_index1 = find(y(start_idx:end_idx) >= half_max, 1, 'first') +
start_idx;
    half_index2 = find(y(start_idx:end_idx) >= half_max, 1, 'last') +
start_idx;
    fwhmx = x(half_index2) - x(half_index1);
```

```
    % translate data to get new baseline y-value
    y_sub = y_sub - y(start_idx);
    area = trapz(x_sub, y_sub);

    % print results
    fprintf("----------------------------\n");
    fprintf("start: (%d, %d)\n", x_start, y_start);
    fprintf("end: (%d, %d)\n", x_end, y_end);
    fprintf("area under curve: %d\n", area);
    fprintf("full width half max: %d\n", fwhmx);
    fprintf("absolute peak height: %d\n", peak_height);
    fprintf("relative peak height: %d\n", peak_height - y(start_idx));
    fprintf("----------------------------\n");
end
```

Appendix C. Previous Work in Aneuploidy Project (Unpublished)

This work was completed by Adriana Coll De Peña and Jennifer Pollock.

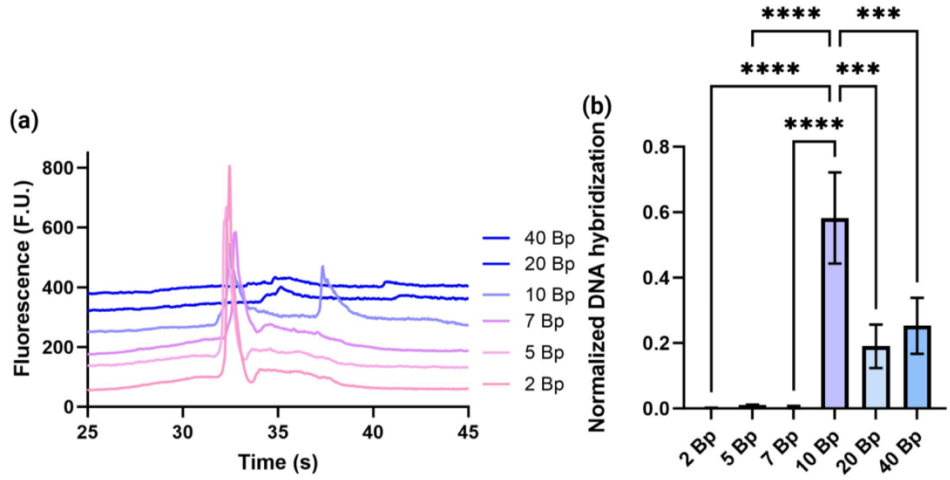

Figure C - 1. (a) Electropherogram representative of the binding efficiency for fully hybridized product with complimentary overhanging binding regions that vary in length. (b) Ratio of the average area under the electropherogram

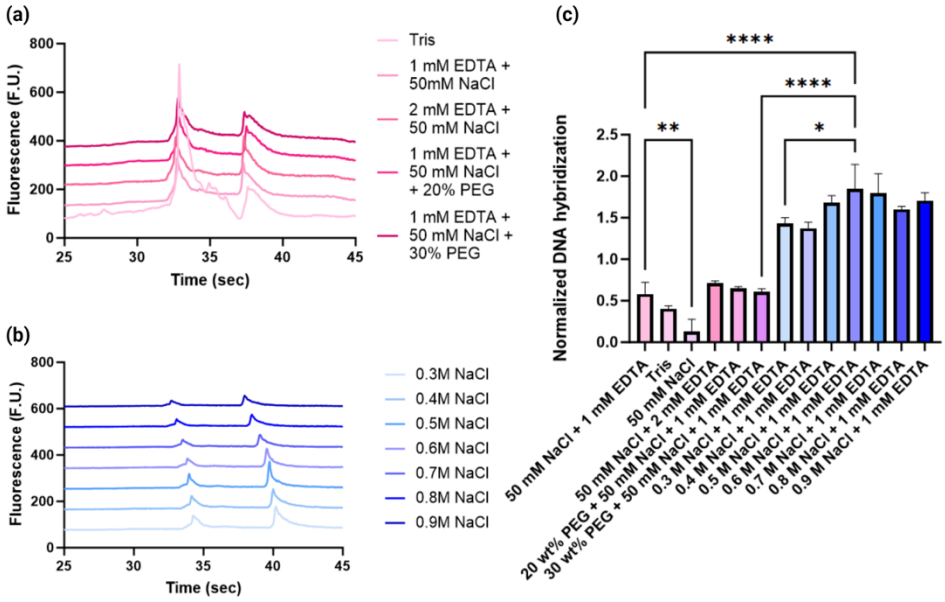

Figure C - 2. (a) Electropherogram representative of the binding efficiency for fully hybridized product prepared with sample buffers with varying components. (b) Electropherogram representative of the binding efficiency for fully hybridized product prepared with sample buffers of varying sat concentration. (c) Ratio of the average area under the electropherogram.

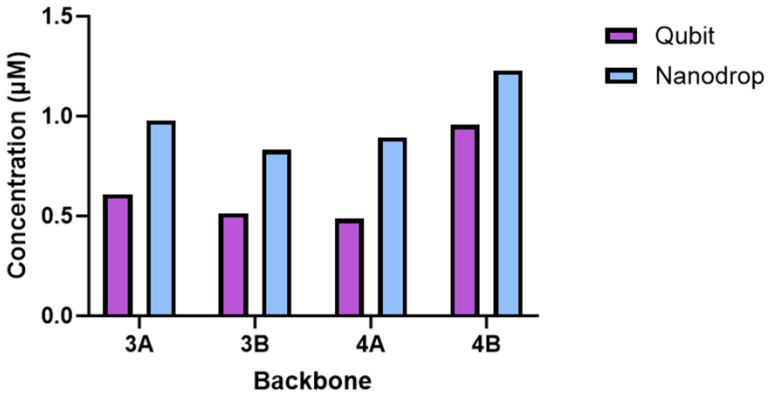

Figure C - 3. Difference in concentration between DNA backbones measured with Qubit vs. NanoDrop.

Appendix D. Coursework

I carefully selected my courses to focus my master's on women's reproductive health and research. My five classroom courses accomplished this and increased my technical competencies in biology and engineering, specific to women's reproductive health. The remaining three course units were used towards research through ENGN 2980.

- BIOL 2300: Biomolecular Interactions
- PHP 2220F: Reproductive & Perinatal Epidemiology
- BIOL 1330: Biology of Reproduction
- ENGN 1510: Nanoengineering & Nanomedicine
- ENGN 2920G: Creating Economic and Social Value from Your Science or Engineering Research

In each of these courses, I took advantage of project assignments to learn something new in women's reproductive health. In doing this, I was able to gain a comprehensive background in a range of topics that went beyond my primary research projects. Project titles are listed below:

- BIOL 2300:
    - Identifying novel interactors of TAF4b in human ovarian granulosa cells. *(grant proposal).*
- PHP 2220F:
    - Lifelong Complications of PCOS. *(paired project, presentation).*
- BIOL 1330:
    - Female to Male Transgender Pregnancy. *(presentation & technical report).*
- ENGN 1510:

- Extracellular vesicles as a nanocarrier platform for the early diagnosis of preeclampsia. *(team project, grant proposal).*

- ENGN 2920G:
  - Wearable Device for Continuous Non-Invasive Hormone Testing. *(paired project, presentation).*
  - Artificial Intelligence in Prenatal Ultrasound. (*technology analysis report & presentation).*